SCIENTIFIC REPORTS

OPEN

SUBJECT AREAS:
CARBON NANOTUBES AND FULLERENES
PHYSICAL CHEMISTRY
SURFACE CHEMISTRY
MATERIALS SCIENCE

Received
24 July 2012

Accepted
13 September 2012

Published
12 October 2012

Correspondence and requests for materials should be addressed to N.N. (nakashima-tcm@mail.cstm.kyushu-u.ac.jp)

Thermodynamics on Soluble Carbon Nanotubes: How Do DNA Molecules Replace Surfactants on Carbon Nanotubes?

Yuichi Kato[1], Ayaka Inoue[1], Yasuro Niidome[1,2] & Naotoshi Nakashima[1,2,3]

[1]Department of Applied Chemistry, Kyushu University, 744 Motooka, Nishi-ku, Fukuoka 819-0395, Japan, [2]International Institute for Carbon Neutral Energy Research (I2CNER), World Premier International Research Center Initiative (WPI), Kyushu University, 744 Motooka, Nishi-ku, Fukuoka 819-0395, Japan, [3]JST-CREST, 5 Sanbancho, Chiyoda-ku, Tokyo 102-0075, Japan.

Here we represent thermodynamics on soluble carbon nanotubes that enables deep understanding the interactions between single-walled carbon nanotubes (SWNTs) and molecules. We selected sodium cholate and single-stranded cytosine oligo-DNAs (dCn (n = 4, 5, 6, 7, 8, 10, 15, and 20)), both of which are typical SWNT solubilizers, and successfully determined thermodynamic properties (ΔG, ΔH and ΔS values) for the exchange reactions of sodium cholate on four different chiralities of SWNTs ((n,m) = (6,5), (7,5), (10,2), and (8,6)) for the DNAs. Typical results contain i) the dC5 exhibited an exothermic exchange, whereas the dC6, 8, 10, 15, and 20 materials exhibited endothermic exchanges, and ii) the energetics of the dC4 and dC7 exchanges depended on the associated chiral indices and could be endothermic or exothermic. The presented method is general and is applicable to any molecule that interacts with nanotubes. The study opens a way for science of carbon nanotube thermodynamics.

Carbon nanotubes (CNTs) are promising nanomaterials for the next generation and from the viewpoints of fundamental science and applications, understanding the thermodynamics of soluble carbon nanotubes is essential. Single-walled carbon nanotubes (SWNTs)[1] are solubilized in solution with the aid of dispersants[2,3] including surfactants[4–8], polycyclic aromatic compounds[9], bio-molecules[7,8,10], and synthetic polymers[11–13]. To develop a systematic understanding of SWNT solubilization, quantitative analysis of the interactions between dispersant molecules and SWNTs is required. Coleman et al. studied the interaction of polymers in the dissociation of SWNT bundles using absorption, fluorescence, and Raman scattering spectrscopy[14]. This was a pioneering piece of work, in that it allowed for quantitative evaluation of the solubilization provided by polymers that had strong interactions with SWNTs. Several studies focused on the chirality sorting of SWNTs have also included analysis of the interactions between SWNTs and dispersants, which were designed to have a strong interaction with a specific chirality (n,m) of the SWNTs[15–17]. Despite enormous efforts focused on efficient chirality sorting, there have only been a few experimental works reported in the literature attempting to quantitatively evaluate the interactions between SWNTs and dispersants. Zhang et al. reported that the base sequence and chain-length of oligo-DNAs affected SWNT-sorting[18] and the *kinetics* of the ssDNA replacement by a surfactant on the surfaces of the (6,5)SWNTs based on the analysis of Eyring's *theory of absolute reaction rates*[19,20]. Molecular adsorption[21–25] and chromatography[26–29] using SWNT-coated silica spheres have been reported as useful methods for assigning the order of interactions between some organic molecules and SWNTs. Molecular dynamic simulations also have been reported to understand the interaction of DNA and SWNTs[30–35]. In this paper, we introduce *thermodynamics* for investigating the interactions between molecules and SWNTs.

Previously, we reported the thermodynamic analysis of an exchange reaction between sodium cholate (SC) and single-stranded oligo-DNA (dC20) on SWNTs[36]. This work provided a preliminary evaluation of the equilibrium constants ($K_{exchange}$), enthalpy changes (ΔH), and entropy changes (ΔS) associated with the exchange reactions. It is assumed that these parameters adequately reflect the differences in the interactions between dispersants and SWNTs. Although our method is simple, it is applicable to any dispersant providing its exchange leads to spectral changes in the SWNT.

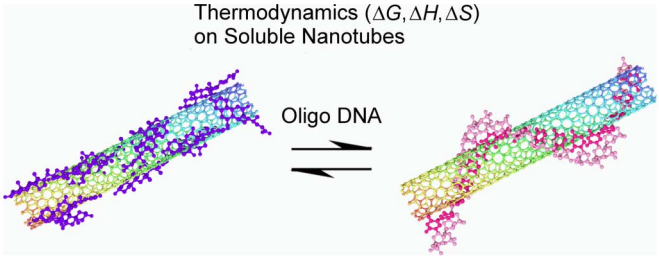

Figure 1 | A schematic drawing of the exchange reaction. The left figure is the SC-dissolved SWNTs and the right figure is the DNA-dissolved SWNTs. Quantitative evaluation of the exchange reaction between SC-dispersed SWNTs and DNA-dissolved SWNTs were performed in this study.

In this study, we describe the thermodynamics of carbon nanotubes in solution for gaining a fundamental understanding of the interaction of dispersant molecules and SWNTs, and emphasize the importance of the presented concept. The introduction of thermodynamics on soluble nanotubes opens the way to a new breed in nanocarbon science. The dispersants used in this study are SC and single-stranded oligo-DNAs, dCn (n = 4, 5, 6, 7, 8, 10, 15, 20). A schematic drawing of the exchange reaction is shown in Fig. 1. The absorption spectra of SWNT solutions containing both SC and dCn were measured at six different temperature conditions, including 15, 20, 25, 30, 35, 40°C. The $K_{exchange}$, ΔH, and ΔS values of the exchange reactions were evaluated using the spectral shifts of the near-IR absorptions for the four chiral indices of the SWNTs ((6,5), (7,5), (10,2), and (8,6)).

Results

Exchange reactions of SC for DNAs on SWNTs. SWNTs (HiPCO) were dispersed in a solution of SC using sonication[36], and the appropriate concentrations of DNA were then added. Twenty-four solutions were prepared in the same way and placed in optical cells with different DNA concentrations ranging from 0 to 1.25 mM. Eight types of DNA were used for this work. Thus, 192 sample solutions were prepared in total, with 24 concentrations for each of the eight different types of DNA (i.e. 24 × 8 = 192). The solutions were kept in optical cells with an optical path length of 1 cm and analysed by absorption spectroscopy using a conventional spectrophotometer (V-670 JASCO). Spectral changes in the solutions following their preparation ceased to occur within 72 h at 15°C (Supplementary Figs. S1, S2). The absorption spectra of the sample solutions were also obtained at five different temperatures, including 20, 25, 30, 35, and 40°C. In each case, the solutions were held at their respective temperatures for about 24 h prior to the measurements. All of the spectra were recorded at the six different temperatures (i.e. 192 × 6 = 1,152 spectra) (Supplementary Figs. S3–S10). For both the solutions before and after addition of the DNAs, the SWNTs were individually solubilized in water by the aid of the adsorbents; namely, we observed typical AFM images of wrapped SWNTs (Supplementary, Fig. S11).

Typical absorption spectra of the SC-dispersed SWNTs in the absence and presence of the DNAs (dC5 (a) and dC20 (b)) at 25°C are shown in Fig. 2. The absorption peaks are due to the S11 transitions of the semiconducting SWNTs[37]. It is evident that the addition of the DNA oligomers caused a red shifting of the peaks in the spectra[38–40]. The spectral changes could be attributed to the changes in the dielectric environments around the SWNTs caused by the exchange of SC for the oligomers on the SWNTs[38–40]. In this study, only four different SWNTs with (n,m)=(6,5), (7,5), (10,2), and (8,6) enabled thermodynamics treatment; namely, the S11 transition bands shown in Fig. 2 are due to corresponding each (n,m)-chirality. Due to absorption peak overlapping, thermodynamics on the SWNTs with other (n,m)chiralities, such as (8,4)-, (7,6)-, and (9,4)SWNTs that were observed around 1145 nm, were unable to conduct. Existence of isosbestic points that are observed in Fig. 2 indicates that thermodynamic analysis enables for the exchange reactions by using a two-states model, in which one state is the SC-dispersed SWNTs and the another is the DNA-dispersed SWNTs[36]. The intermediate states where SC and the DNAs simultaneously affected the photoabsorption of the SWNTs are not observed under our experimental conditions.

Equilibrium constants. Fractions of the SC-dispersed SWNTs and DNA-dispersed SWNTs are denoted as θ_{SC} and θ_{DNA}, respectively. The spectral changes in Figs. 2 and S3–S10 enable the evaluation of

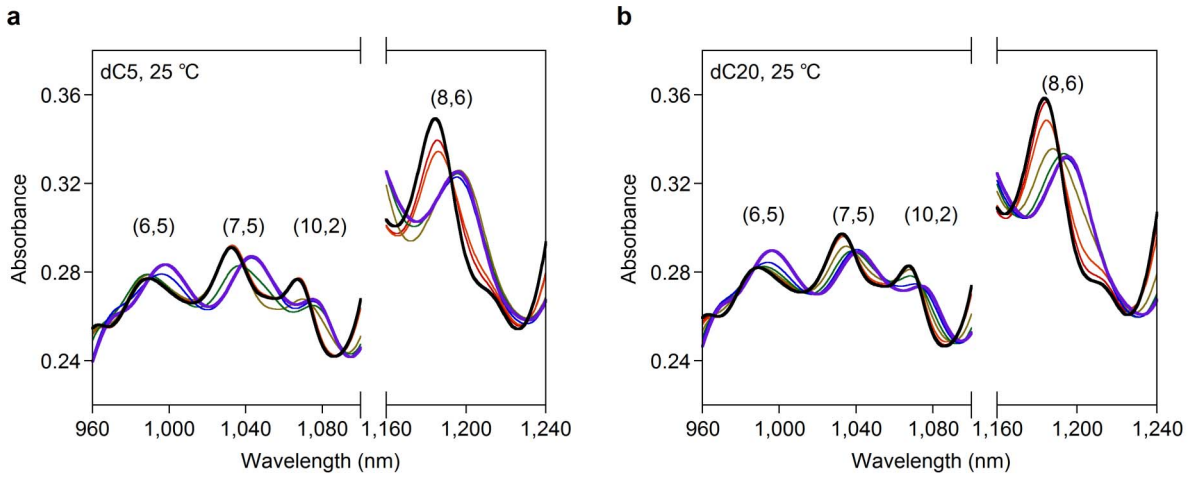

Figure 2 | Absorption spectra of the SWNT in the mixed solution of SC and DNA. Absorption spectra of the SC-dispersed SWNT solutions in the absence (thick black line) and presence (coloured lines) of dC5 (a) and dC20 (b). The concentrations of dC5 were 0 (black), 28.1 (red), 31.3 (orange), 156 (yellow), 313 (green), 781 (blue), and 1,250 μM (purple). The concentrations of dC20 were 0 (black), 0.0625 (red), 0.156 (orange), 0.313 (yellow), 0.469 (green), 0.938 (blue), and 15.6 μM (purple). The temperature was 25°C. The pair of integers (n,m) written above the peak tops indicate the chiral indices of the SWNTs. The spectral changes are attributed to the exchange of SC for the DNAs on the SWNTs (ref 32–34). Isosbestic points were observed in the spectral changes. The exchange reactions could be analysed using a two-states model, in which one state is the SC-dispersed SWNTs and the other is the DNA-dispersed SWNTs.

θ_{DNA}. Based on the two-states model, the changes in absorbance at 1,000, 1,030, 1,081, and 1,183 nm were assumed to be proportional to the θ_{DNA} values of (6,5), (7,5), (10,2), and (8,6), respectively. The evaluation was performed for the all absorption spectra, providing 4,608 θ_{DNA} values from the 1,152 spectra (i.e. 1,152 × 4 chiralities = 4,608). A plot of θ_{DNA} at 25°C versus the concentration of the DNA oligomers on a logarithmic scale is shown in Fig. 3. The θ_{DNA} values of the five different types of oligomers (dC5, 8, 10, 15, and 20) presented in the figure were selected to highlight the typical changes of θ_{DNA} depending on the DNA concentrations. The total number of θ_{DNA} plots is actually 192 (i.e. 4 chiralities × 6 temperatures × 8 DNAs = 192) (For all θ_{DNA} plots, see Supplementary Figs. S12–S14). These θ_{DNA} plots clearly show the courses of the exchange reactions of SC with DNA on the respective (n,m) SWNTs. Equilibrium constants for the exchanges of SC with the oligomers ($K_{exchange}$) were obtained by fitting the θ_{DNA} plots using Equation (1), which was based on the Hill Equation:

$$Absorbance = A_1 + A_2\theta_{DNA} = A_1 + A_2 \frac{[DNA]^n}{\left(\frac{[SC]}{K_{exchange}}\right)^n + [DNA]^n} \quad (1)$$

where A_1 is the absorbance of the SC-SWNTs, A_2 is the difference in the absorbance between the DNA-SWNTs and the SC-SWNTs, and n is the Hill coefficient reflecting the cooperativity of the exchanges. The lines in Fig. 3 are the fitting lines generated by equation (1). The fitting of the 192 θ_{DNA} plots (Supplementary Figs. S12–14) gave the corresponding 192 $K_{exchange}$ values. It is clear that the experimental results and the fitting curves were in good agreement. Some of the $K_{exchange}$ values obtained at 25°C using the five kinds of oligomers (dC5, 8, 10, 15, 20) are listed in Table 1. (For all of the $K_{exchange}$ values and the corresponding Hill coefficients (n), see Supplementary Tables S1 and S2).

The $K_{exchange}$ values of the four different chiral-types of the SWNTs at 25 and 35°C plotted against the length of the DNA are shown in Fig. 4 (for plots at the four other temperatures of 15, 20, 30, and 40°C, see Supplementary Fig. S15). We will discuss interesting DNA chain length dependence later.

Thermodynamic parameters. The temperature dependence of the $K_{exchange}$ value was examined to obtain the thermodynamic parameters of the exchange reactions. Plots depicting the relationship between $\ln K_{exchange}$ and 1/T for the exchange reactions between SC and three different DNAs (dC5, 10, and 20) on the SWNTs with four specified chiral indices are shown in Fig. 5 (for the results using dC4, 6, 7, 8, and 15, see Supplementary Fig. S16). It is clear from Fig. 5 that the plots of $\ln K_{exchange}$ versus 1/T exhibit good linear relationships. The results could therefore be analysed using equation (2), allowing the relationship between the $K_{exchange}$ and Gibbs energy changes (ΔG) to be formulated.

$$-RT \ln K_{exchange} = \Delta G = \Delta H - T\Delta S \quad (2)$$

As a result of the line fitting, the enthalpy and entropy changes (ΔH and ΔS) for the exchange reactions were successfully evaluated. The

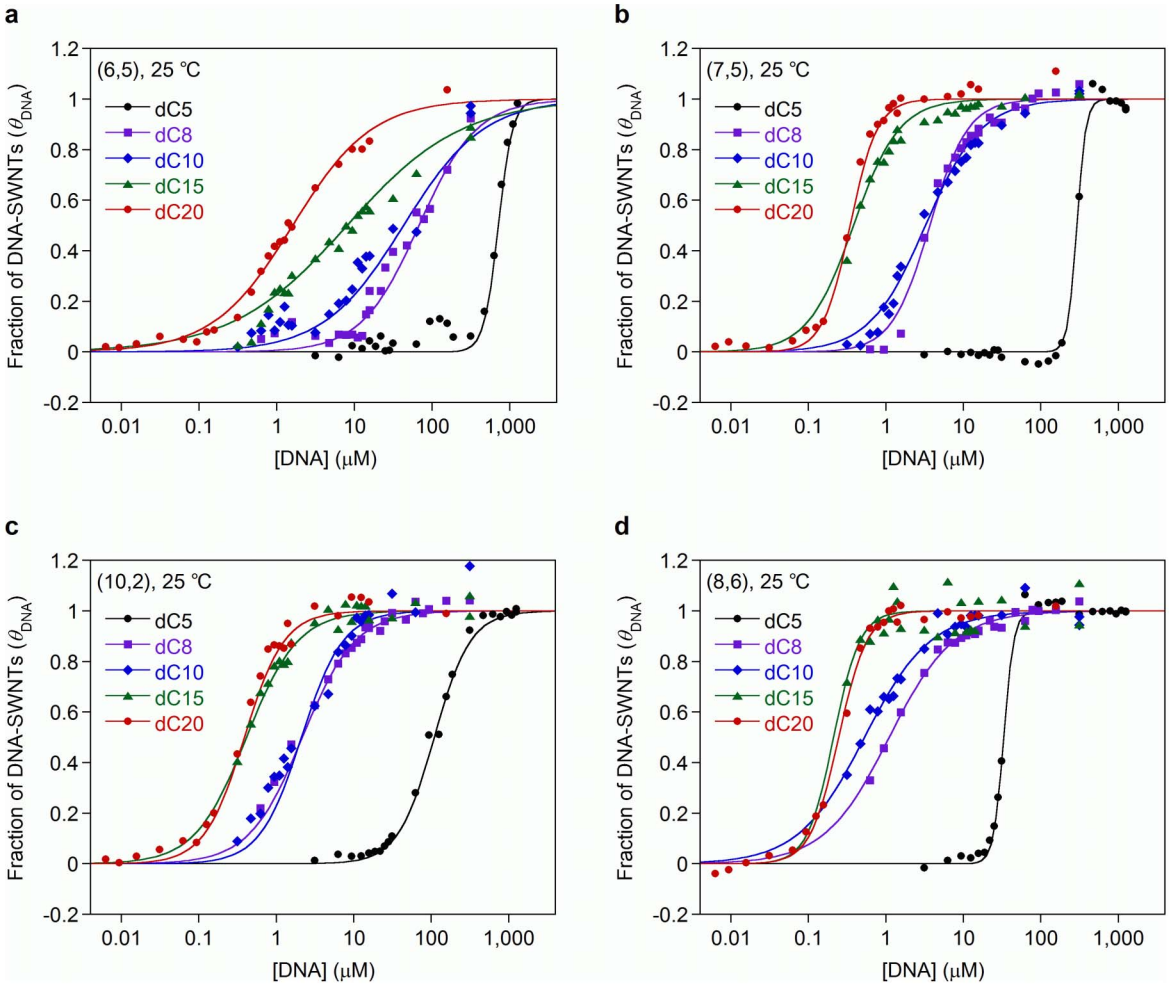

Figure 3 | Fractions of DNA-SWNTs (θ_{DNA}) in the SC solutions as a function of concentration of dCn. Lines fitted by Equation (1). The four kinds of SWNTs were a: (6,5), b: (7,5), c: (10,2), and d: (8,6). The temperature was 25°C.

Table 1 | Equilibrium constants and the thermodynamic parameters of the exchanges. Equilibrium constants for the exchange of SC for DNA on SWNTs with different chiral indices at 25°C. The thermodynamic parameters ΔG, ΔH, ΔS, and $T\Delta S$ are also presented for the exchange reactions and were obtained from linear analyses of the 1/T plots (equation (2))

Chiral index	Diameter (nm)		$K_{exchange}$ (25°C)	ΔG (kJ/mol)	ΔH (kJ/mol)	ΔS (J/mol K)	$T\Delta S$ (kJ/mol)
(6,5)	0.76	dC5	2.73±0.14	−2.42±0.18	−17.4±1.7	−50.1±5.6	−14.9±1.7
		dC8	28.8±7.3	−8.28±0.65	1.47±3.52	32.7±11.7	9.76±3.49
		dC10	45.5±8.2	−9.03±0.45	17.1±4.77	87.7±15.9	26.2±4.7
		dC15	406±95	−14.4±0.4	25.5±7.3	134±24	39.9±7.3
		dC20	1,260±140	−17.6±0.1	34.5±2.1	175±7	52.1±2.1
(7,5)	0.83	dC5	6.66±0.11	−4.89±0.50	−31.0±3.4	−87.7±11.4	−26.1±3.4
		dC8	526±42	−15.1±0.1	10.1±5.5	84.3±18.3	25.1±5.5
		dC10	600±54	−15.8±0.2	17.9±2.1	113±7	33.6±2.0
		dC15	5,260±280	−21.1±0.1	12.1±1.8	112±6	33.3±1.8
		dC20	5,810±210	−21.5±0.1	4.14±0.29	85.9±0.9	25.6±0.3
(10,2)	0.88	dC5	17.8±0.6	−6.91±0.18	−22.1±3.0	−50.9±9.9	−15.2±3.0
		dC8	897±43	−16.7±0.2	15.5±2.4	108±8	32.2±2.4
		dC10	918±130	−17.2±0.2	17.9±5.5	118±18	35.1±5.5
		dC15	4,870±330	−21.0±0.1	6.68±0.92	92.9±3.1	27.7±0.9
		dC20	5,430±269	−21.3±0.1	10.4±1.1	106±4	31.7±1.1
(8,6)	0.97	dC5	58.5±1.1	−10.1±3.8	−32.0±3.3	−73.3±11.1	−21.9±3.3
		dC8	1,760±100	−18.6±1.1	28.9±7.8	160±26	47.6±7.8
		dC10	3,670±330	−20.4±0.8	26.3±6.0	157±19.8	46.7±5.9
		dC15	9,480±2610	−21.9±1.1	5.33±3.66	94.2±12.2	28.1±3.6
		dC20	8,160±300	−22.3±0.1	1.92±1.11	81.2±3.7	24.2±1.1

fitting treatments for the four different chiralities of SWNTs and the eight different dCn types provided 32 sets of ΔG, ΔH and ΔS values. Typical results are tabulated in Table 1 (for other data, see Supplementary Table S3). As shown by the positive slopes shown in Fig. 5a, the exchange reactions of SC with dC5 are exothermic for all of the different chirality-types of the SWNTs. In contrast, the negative slopes shown in Fig. 5b,c indicate that the exchanges of dC10 (b) and dC20 (c) are endothermic. In addition, it was revealed that the (6,5)SWNTs have different $K_{exchange}$ values from those of the other SWNTs.

Fig. 6 shows the ΔH and ΔS values plotted against the chain length of dCn (n = 4–20). A negative ΔH value indicates an *exothermic* reaction. Exothermic reactions were found for the following exchange reactions: i) reactions using dC5 for the SWNTs with the four specified (n,m)SWNTs, ii) reactions using dC4 for the (7,5)- and (8,6) SWNTs, and iii) reactions using dC7 for the (6,5)- and (7,5)SWNTs. All of the other exchange reactions showed positive ΔH values, indicating that they are endothermic processes. The ΔS values also reflected a similar tendency, in that the ΔS values are negative in the following cases: i) reactions using dC5 for the SWNTs with the four specified (n,m)SWNTs, ii) reactions using dC4 for the (7,5)-, (10,2)- and (8,6)SWNTs, iii) reactions using dC7 for the (7,5)SWNTs. All of the other exchange reactions showed positive ΔS values, indicating that the spontaneous exchanges were being driven by the entropy changes. The ΔS and ΔH values are all positive for the four (n,m) SWNTs when longer DNAs (≥ dC8) were used. It has been revealed that the exchange reactions using DNAs longer than dC8 are entropy-driven reactions.

Discussion

The obtained results shown in Figs. 4 and S15 demonstrate two interesting features, the first of which is that the $K_{exchange}$ values

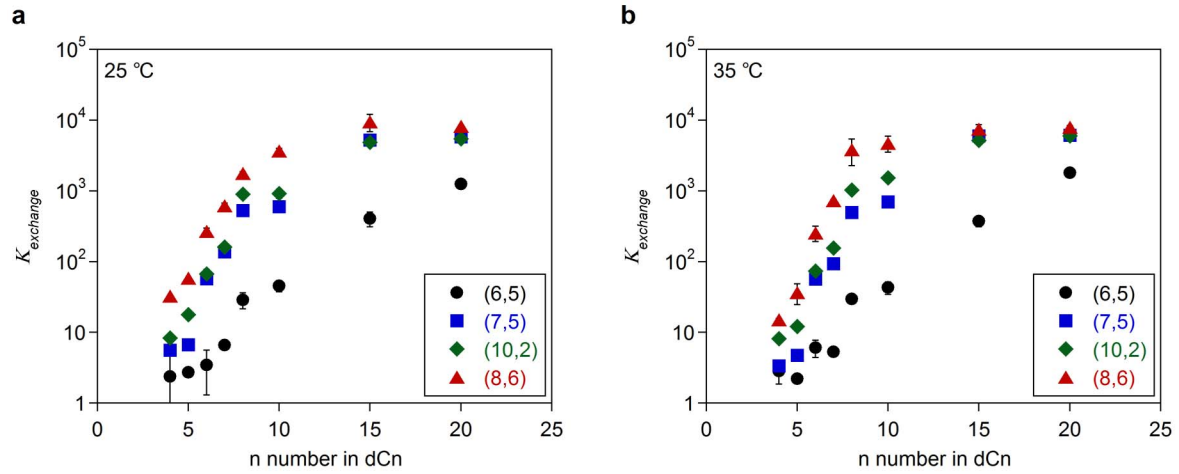

Figure 4 | Chain-length dependence of equilibrium constants (Kexchange). The $K_{exchange}$ for the exchange of SC for the dCn on the (n,m)SWNTs (n,m=(6,5), (7,5), (10,2) and (8,6)) at 25°C (a) and 35°C (b). The $K_{exchange}$ values exhibited a strong dCn-molecular weight dependence, which means dCn materials with larger n numbers induced the spectral changes at the lower DNA concentration. The SWNTs with larger diameters tended to show larger $K_{exchange}$ values. The order of the diameters for the four different chirality-types of the SWNTs was (6,5): 0.76 nm < (7,5): 0.83 nm < (10,2): 0.88 nm < (8,6): 0.97 nm.

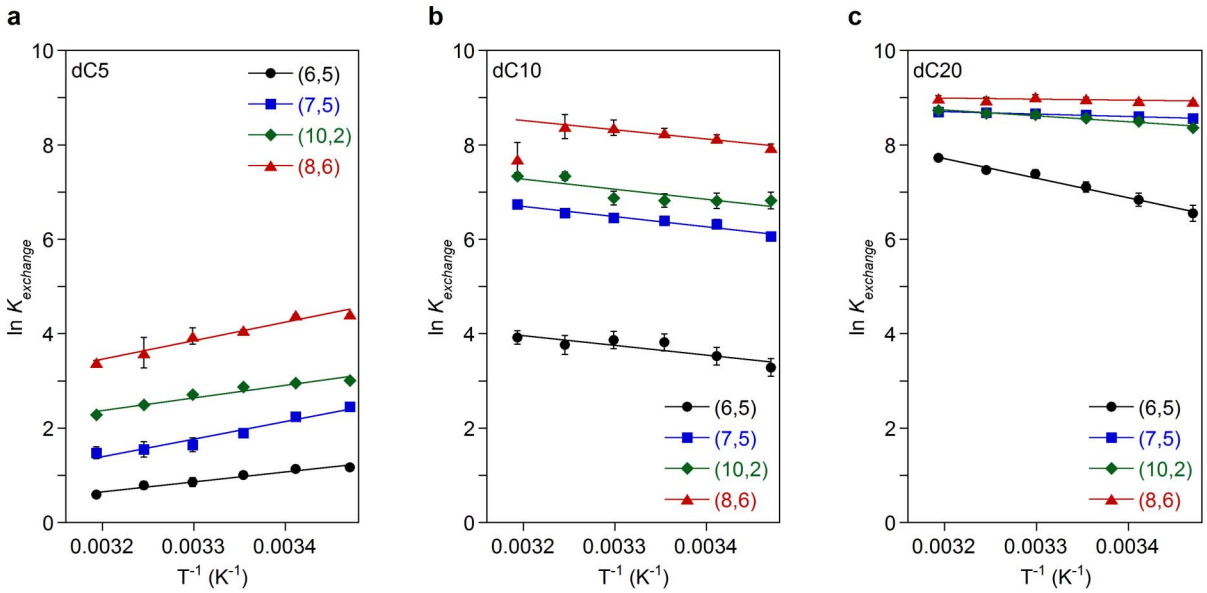

Figure 5 | Temperature dependence of the Kexchange. 1/T plots of the exchange of SC for dC5 (a), dC10 (b) and dC20 (c) on SWNTs. The chiral indices of the SWNTs were (6,5) (black), (7,5) (blue), (10,2) (green), and (8,6) (red).

exhibited a strong dCn-molecular weight dependence. This observation is consistent with the results shown in Fig. 3, in which the dCn materials with larger n numbers induced spectral changes at a lower DNA concentration. The plots in Figs. 4 and S15 revealed the same tendencies for all of the chiral indices across all of the temperatures studied. With the exception of the (6,5)SWNTs, the log$K_{exchange}$ values increased in an almost linear fashion with an increase in the number oligomer residues (n = 4–10) and reached almost constant values at n = 10, 15, and 20. For the (6,5)SWNTs, in the range of n = 4–20, the log$K_{exchange}$ values increased in an almost linear fashion with an increase in the number of residues, which is rational considering the nature of molecular interaction between the adsorbents and the nanotube surfaces.

The second interesting feature of the data is that the SWNTs with larger diameters tended to show larger $K_{exchange}$ values. The order of the diameters for the four different chiral-types of the SWNTs was (6,5): 0.76 nm < (7,5): 0.83 nm < (10,2): 0.88 nm < (8,6): 0.97 nm. The $K_{exchange}$ values of dC10 were 45.5, 600, 918 and 3,670 for the (6,5), (7,5), (10,2) and the (8,6)SWNTs, respectively. This order was independent of the different lengths of oligomers and the temperatures used. The $K_{exchange}$ of value the (6,5)SWNTs was found to be remarkably small relative to those of SWNTs with other chiral indices. The exchange processes of SC with the DNA oligomers on the (6,5)SWNTs could potentially have different characteristics from the other chiral-types. It has been revealed, therefore, that the interactions of SC and DNA oligomers with SWNTs are sensitive to small differences in the diameters of the SWNTs.

The results shown in Fig. 6 indicated that the longer DNAs provided larger positive ΔS values, which compensate the endothermic ΔH term. In comparison, the shorter DNAs provided negative entropy changes when they replaced the SC molecules on the SWNTs. The negative ΔH values for the shorter DNAs reflected the difference in the interaction energies between the SC-SWNTs and DNA-SWNTs. When the DNAs do not have intense entropy changes with the SC-DNA (i.e. when the length of the DNA was short), the enthalpy change became the dominant driving force for the exchange reactions between SC and the oligomers. (Plots of ΔH vs. ΔS for the four (n,m)SWNTs show linear relations due to ΔH-ΔS compensation on the present exchange reaction (see Supplementary Fig. S17)).

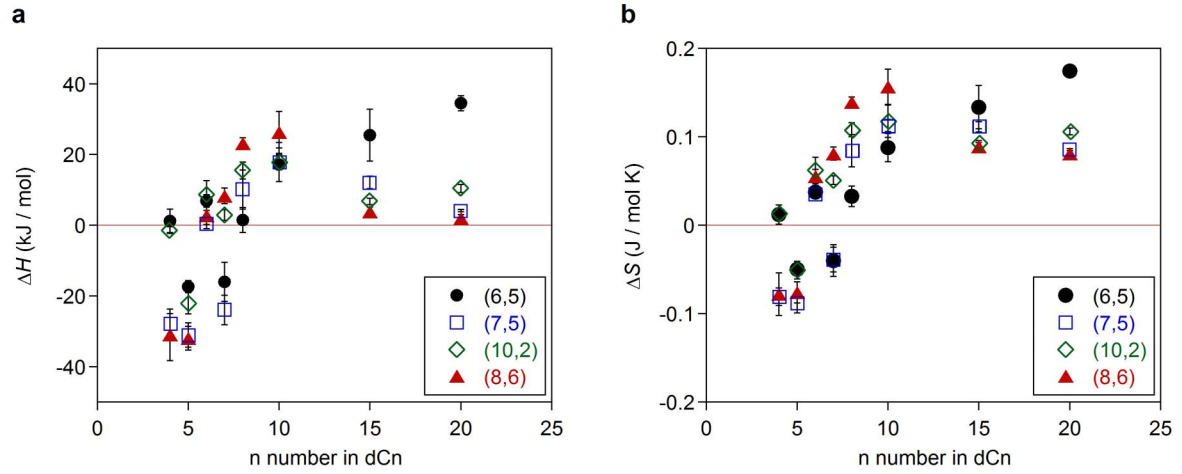

Figure 6 | Chain-length dependence of thermodynamic parameters. Thermodynamic parameters for the exchanges of SC with dCn on SWNTs with different chiral indices. a: enthalpy changes (ΔH) and b: entropy changes (ΔS).

The DNA-length dependence was somewhat complicated. A discussion of the results for the (7,5)-, (10,2)- and (8,6)SWNTs will be provided first because the result for the (6,5)SWNTs were different from the others. When the DNA was longer than dC8, larger positive ΔH and ΔS values were obtained for the three (n,m)SWNTs. The dC10 material gave the largest ΔH and ΔS values, with the exchange reaction in this case being entropy-driven. Oligomers longer than dC10 provided smaller but still positive ΔH and ΔS values, and the (8,6)SWNTs gave very small positive ΔH values when dC20 was used for the exchanges. The ΔS value for dC20 was still positive, but the magnitude of the ΔS value was smaller than that observed for dC10. The longer DNA chains of dC15 and dC20 could interact with each other through electrostatic repulsive forces on SWNT, leading to a decrease in the enthalpy and entropy changes. In contrast, the (6,5)SWNTs showed different characteristics, with the longer DNA providing larger positive ΔH and ΔS values than those observed when dC7 was used. The dC20 gave the largest ΔH and ΔS values. The smaller diameter of the (6,5)SWNTs must have affected the interactions between the (6,5)SWNT and the DNAs.

The dependence of the thermodynamic parameters of solubilizing SWNTs with DNA oligomers on the diameter is clearly a complicated relationship. In the cases of dC4 and dC7, the chiral indices affected whether the exchange reactions were exo- or endothermic. In the cases of dC7, dC8 and dC10, SWNTs with a larger diameter tended to show larger positive ΔH and ΔS values. In contrast, in the case of dC15 and dC20, SWNTs with smaller diameters tended to show larger positive ΔH and ΔS values. No information pertaining to the microscopic structures of SC and the DNAs on the SWNTs was collected during the current study. These thermodynamic parameters, however, reveal the complicated interplay between the diameter of SWNTs and the size of dispersants during the solubilizing process.

To conclude, we have described that a basic thermodynamic treatment is applicable to soluble carbon nanotubes. This analytical method provides a new platform for deep understanding the interactions of molecules with the nanotubes. In this study, the method was applied to the exchange reactions of SC and DNAs, and revealed that longer DNAs showed larger $K_{exchange}$ values and the exchange reactions involving the DNAs longer than dC8 were entropy-driven, whereas exchange reactions involving DNAs shorter than dC8 were enthalpy-driven for most of the chiral indices investigated. These results are plausible, especially when considered from the perspective of the entropy changes associated with the exchanges. Although SWNTs with larger diameters tended to show larger $K_{exchange}$ values, the general dependence of the thermodynamic parameters of the SWNTs on the diameter was complicated.

These quantitative data could contribute to the development of sophisticated molecular dynamics simulations. Furthermore, this research could also provide a platform for the development of a new thermodynamic understanding of the surfaces on nanomaterials because the present technique provides a general method that can be applicable to many molecules that interact and cause a spectral shift of nanotubes; indeed, similar spectral shifts were observed when sodium dodecyl sulphate, sodium dodecylbenzene sulphonate, or sodium deoxy cholate was used in place of SC (Supplementary, Fig. S18). The presented thermodynamics analysis provides deep understanding the interactions of molecules and nanotubes, and such fundamental analysis might be useful for practical applications, such as thermo-triggered DNA gene delivery systems, biosensors and self-assembly of molecules on carbon nanotubes.

Methods

Materials and solubilization of SWNTs. Purified SWNTs (HiPco-SWNTs) were purchased from Unidym Co. Sodium cholate (SC), anhydrous disodium hydrogen phosphate and sodium hydroxide were purchased from Kishida Chemical. Oligo-DNAs (single-stranded 4, 5, 6, 7, 8, 10, 15 and 20-mer cytosine, denoted dCn) were purchased from Hokkaido System Science. The experimental conditions used to obtain dispersed SWNTs (SC-SWNT solutions) were the same as those reported in our previous papers[36]. Thus, SWNTs (6 mg) were dispersed in 15 mL of an SC micellar solution (4 mM) by sonication (bath-type sonicator, BRANSON5510) for 1 h. The resulting solution was then centrifuged at 120,000 *g* (Hitachi-Himac CS150GXL equipped with a swinging bucket rotor S55A (Hitachi High-Technologies Corporation)) for 2 h, and the top 80% of the supernatant was collected for measurements.

SC-DNA exchange reactions. The SC-SWNT solutions, DNA solutions, and buffer solutions were mixed for the chain-length dependence experiment. The concentration of SC was adjusted to 2 mM using a dialysis membrane (MWCO: 10,000). All of the solutions contained a phosphate buffer solution (pH= 11.5, 20 mM). The DNA concentration was adjusted from 0 to 1.25 mM. The solutions were stored for 3 days at 15°C and then for 1 day at specified temperatures (20, 25, 30, 35, or 40°C) to reach equilibrium states. Absorption spectra were measured using a V-670 spectrophotometer (JASCO) equipped with a temperature controller (ETCS-761).

Thermodynamics. Thermodynamics on the SC-DNA exchange reactions are described in the main body.

DNA-Surfactants exchange reactions. The DNA-SWNT solutions, surfactants (sodium dodecyl sulphate, sodium dodecylbenzene sulphonate, and sodium deoxy cholate) solutions. and buffer solutions were mixed. The concentration of DNA (dC20) was adjusted to 4 μM. All of the solutions contained a phosphate buffer solution (pH= 11.5, 20 mM). The concentrations of surfactants were adjusted from 0 to 10 mM. The solutions were stored for 1 day at 25°C to reach equilibrium states. Absorption spectra were measured equipped with a temperature controller.

AFM measurements. The SC-SWNT solutions in the absence and presence of dC20 (15.6 μM) were demineralized. The solutions were casted on mica substrates. Nanostructure images were taken using an atomic force microscope (PicoPlus 5500, Agilent Technologies, Inc.).

1. Iijima, S. & Ichihashi, T. Single-shell carbon nanotubes of 1-nm diameter. *Nature* **363**, 603–605 (1993).
2. Nakashima, N. & Fujigaya, T. Fundamentals and applications of soluble carbon nanotubes. *Chem. Lett.* **36**, 692–697 (2007).
3. Fujigaya, T. & Nakashima, N. Methodology for homogeneous dispersion of single-walled carbon nanotubes by physical modification. *Polym. J.* **40**, 577–589 (2008).
4. O'Connell, M. J. *et al.* Band gap fluorescence from individual single-walled carbon nanotubes. *Science* **297**, 593–6 (2002).
5. Moore, V. C. *et al.* Individually suspended single-walled carbon nanotubes in various surfactants. *Nano Lett.* **3**, 1379–1382 (2003).
6. Wenseleers, W. *et al.* Efficient isolation and solubilization of pristine single-walled nanotubes in bile salt micelles. *Adv. Funct. Mater.* **14**, 1105–1112 (2004).
7. Ishibashi, A. & Nakashima, N. Individual dissolution of single-walled carbon nanotubes in aqueous solutions of steroid or sugar compounds and their Raman and near-IR spectral properties. *Chem. Eur. J.* **12**, 7595–602 (2006).
8. Duque, J. G. *et al.* Diameter-dependent solubility of single-walled carbon nanotubes. *ACS nano* **4**, 3063–72 (2010).
9. Nakashima, N., Tomonari, Y. & Murakami, H. Water-soluble single-walled carbon nanotubes via noncovalent sidewall-functionalization with a pyrene-carrying ammonium ion. *Chem. Lett.* 638–639 (2002).
10. Zheng, M. *et al.* DNA-assisted dispersion and separation of carbon nanotubes. *Nature Mater.* **2**, 338-42 (2003).
11. Chen, F., Wang, B., Chen, Y. & Li, L.-J. Toward the extraction of single species of single-walled carbon nanotubes using fluorene-based polymers. *Nano Lett.* **7**, 3013–7 (2007).
12. Nish, A., Hwang, J.-Y., Doig, J. & Nicholas, R. J. Highly selective dispersion of single-walled carbon nanotubes using aromatic polymers. *Nature Nanotech.* **2**, 640–6 (2007).
13. Ozawa, H. *et al.* Rational concept to recognize/extract single-walled carbon nanotubes with a specific chirality. *J. Am. Chem. Soc.* **133**, 2651–2657 (2011).
14. Coleman, J. N. *et al.* Binding kinetics and SWNT bundle dissociation in low concentration polymer−nanotube dispersions. *J. Phys. Chem. B* **108**, 3446–3450 (2004).
15. Hersam, M. C. Progress towards monodisperse single-walled carbon nanotubes. *Nature Nanotech.* **3**, 387–94 (2008).
16. Liu, C.-H. & Zhang, H.-L. Chemical approaches towards single-species single-walled carbon nanotubes. *Nanoscale* **2**, 1901–18 (2010).
17. Tanaka, T., Liu, H., Fujii, S. & Kataura, H. From metal/semiconductor separation to single-chirality separation of single-wall carbon nanotubes using gel. *Phys. Status Solidi RRL* **5**, 301–306 (2011).
18. Tu, X., Manohar, S., Jagota, A. & Zheng, M. DNA sequence motifs for structure-specific recognition and separation of carbon nanotubes. *Nature* **460**, 250–3 (2009).
19. Roxbury, D., Jagota, A. & Mittal, J. Sequence specific self-stitching motif of short single-stranded DNA on a single-walled carbon nanotube. *J. Am. Chem. Soc.* **133**, 13545–13550 (2011).

20. Roxbury, D., Tu, X., Zheng, M. & Jagota, A. Recognition ability of DNA for carbon nanotubes correlates with their binding affinity. *Langmuir* **27**, 8282–93 (2011).
21. Debnath, S., Cheng, Q., Hedderman, T. G. & Byrne, H. J. Comparative study of the interaction of different polycyclic aromatic hydrocarbons on different types of single-walled carbon nanotubes. *J. Phys. Chem. C* **114**, 8167–8175 (2010).
22. Debnath, S., Cheng, Q., Hedderman, T. G. & Byrne, H. J. A study of the interaction between single-walled carbon nanotubes and polycyclic aromatic hydrocarbons: toward structure−property relationships. *J. Phys. Chem. C* **112**, 10418–10422 (2008).
23. Gotovac, S. *et al.* Effect of nanoscale curvature of single-walled carbon nanotubes on adsorption of polycyclic aromatic hydrocarbons. *Nano Lett.* **7**, 583–7 (2007).
24. Sano, M., Kamino, A. & Okamura, J. Noncovalent self-assembly of carbon nanotubes for construction of "Cages." *Nano Lett.* **2**, 531–533 (2002).
25. Yoo, J., Fujigaya, T. & Nakashima, N. Facile evaluation of interactions between carbon nanotubes and phthalocyanines using silica spheres coated with ultrathin-layers of single-walled carbon nanotubes. *Chem. Lett.* **40**, 538–539 (2011).
26. Yoo, J., Ozawa, H., Fujigaya, T. & Nakashima, N. Evaluation of affinity of molecules for carbon nanotubes. *Nanoscale* **3**, 2517–22 (2011).
27. Menna, E. *et al.* Carbon nanotubes on HPLC silica microspheres. *Carbon* **44**, 1609–1613 (2006).
28. Chang, Y. X., Zhou, L. L., Li, G. X., Li L. & Yuan, L. M. Single-wall carbon nanotubes used as stationary phase in HPLC. *J. Liq. Chromatogr. Relat. Technol.*, **30,** 2953–2958 (2007).
29. Li, Y. *et al.* Incorporation of single-wall carbon nanotubes into an organic polymer monolithic stationary phase for mu-HPLC and capillary electrochromatography. *Anal. Chem.* **77**, 1398–406 (2005).
30. Gao, H. & Kong, Y. Simulation of DNA-Nanotube Interactions. *Annu. Rev. Mater. Res.* **34**, 123–150 (2004).
31. Manohar, S., Tang, T. & Jagota, A. Structure of Homopolymer DNA-CNT Hybrids. *J. Phys. Chem. C* **111**, 17835–17845 (2007).
32. Johnson, R. R., Johnson, A. T. C. & Klein, M. L. Probing the structure of DNA-carbon nanotube hybrids with molecular dynamics. *Nano Lett.* **8**, 69–75 (2008).
33. Martin, W., Zhu, W. & Krilov, G. Simulation study of noncovalent hybridization of carbon nanotubes by single-stranded DNA in water. *J. Phys. Chem. B* **112**, 16076–89 (2008).
34. Karachevtsev, M. V. & Karachevtsev, V. A Peculiarities of homooligonucleotides wrapping around carbon nanotubes: molecular dynamics modeling. *J. Phys. Chem. B* **115**, 9271–9 (2011).
35. Xiao, Z. *et al.* Base-and Structure-Dependent DNA Dinucleotide-Carbon Nanotube Interactions: Molecular Dynamics Simulations and Thermodynamic Analysis. *J. Phys. Chem. C* **115**, 21546–21558 (2011).
36. Kato, Y., Niidome, Y. & Nakashima, N. Thermodynamics of the exchange of solubilizers on single-walled carbon nanotubes. *Chem. Lett.* **40**, 730–732 (2011).
37. Bachilo, S. M. *et al.* Structure-assigned optical spectra of single-walled carbon nanotubes. *Science* **298**, 2361–6 (2002).
38. Jeng, E. S., Moll, A. E., Roy, A. C., Gastala, J. B. & Strano, M. S. Detection of DNA hybridization using the near-infrared band-gap fluorescence of single-walled carbon nanotubes. *Nano Lett.* **6**, 371–5 (2006).
39. Choi, J. H. & Strano, M. S. Solvatochromism in single-walled carbon nanotubes. *Appl. Phys. Lett.* **90**, 223114 (2007).
40. Kim, J. H. *et al.* Raman and fluorescence spectroscopic studies of a DNA-dispersed double-walled carbon nanotube solution. *ACS Nano* **4**, 1060–6 (2010).

Acknowledgments

We thank Professors A. Robertson at Kyushu University for helpful discussions. This work was supported in part by the Global COE Program "Science for Future Molecular Systems" (Kyushu University) and Nanotechnology Network Project (Kyushu-area Nanotechnology Network) from the Ministry of Education, Culture, Sports, Science and Technology, Japan.

Author contribution

N.N., Y.N. and Y.K. conceived and designed the experiments. Y.K. and A.I. carried out the experiments and data analysis. N.N., Y.N. and Y.K. wrote the manuscript. All authors discussed the results and commented on the manuscript.

Additional information

Supplementary information accompanies this paper at http://www.nature.com/scientificreports

Competing financial interests: The authors declare no competing financial interests.

How to cite this article: Kato, Y., Inoue, A., Niidome, Y. & Nakashima, N. Thermodynamics on Soluble Carbon Nanotubes: How Do DNA Molecules Replace Surfactants on Carbon Nanotubes? *Sci. Rep.* **2**, 733; DOI:10.1038/srep00733 (2012).